

Explicit Path CGR: Maintaining Sequence Fidelity in Geometric Representations

Sarwan Ali

Columbia University, Irvine Medical Center
New York, USA
sa4559@cumc.columbia.edu

Abstract

We present a novel information-preserving Chaos Game Representation (CGR) method, also called Reverse-CGR (R-CGR), for biological sequence analysis that addresses the fundamental limitation of traditional CGR approaches - the loss of sequence information during geometric mapping. Our method introduces complete sequence recovery through explicit path encoding combined with rational arithmetic precision control, enabling perfect sequence reconstruction from stored geometric traces. Unlike purely geometric approaches, our reversibility is achieved through comprehensive path storage that maintains both positional and character information at each step. We demonstrate the effectiveness of R-CGR on biological sequence classification tasks, achieving competitive performance compared to traditional sequence-based methods while providing interpretable geometric visualizations. The approach generates feature-rich images suitable for deep learning while maintaining complete sequence information through explicit encoding, opening new avenues for interpretable bioinformatics analysis where both accuracy and sequence recovery are essential.

Keywords

Chaos Game Representation, Biological Sequences, Deep Learning, Sequence Classification, Reversible Encoding

ACM Reference Format:

Sarwan Ali. 2025. Explicit Path CGR: Maintaining Sequence Fidelity in Geometric Representations. In *Proceedings of the 34th ACM International Conference on Information and Knowledge Management (CIKM '25), November 10–14, 2025, Seoul, Republic of Korea*. ACM, New York, NY, USA, 5 pages. <https://doi.org/10.1145/3746252.3760900>

1 Introduction

Biological sequence analysis remains a cornerstone of computational biology, with applications spanning genomics, proteomics, and evolutionary studies. Traditional approaches rely heavily on sequence alignment algorithms and statistical models that often struggle to capture complex patterns inherent in biological data. The Chaos Game Representation (CGR), introduced by Jeffrey [7], offers an elegant geometric approach to sequence visualization by mapping sequences to unique points in 2D space.



This work is licensed under a Creative Commons Attribution-NonCommercial 4.0 International License.

CIKM '25, Seoul, Republic of Korea

© 2025 Copyright held by the owner/author(s).

ACM ISBN 979-8-4007-2040-6/2025/11

<https://doi.org/10.1145/3746252.3760900>

However, classical CGR suffers from a critical limitation: *information loss*. Once a sequence is mapped to its geometric representation, the original sequence cannot be perfectly reconstructed. This irreversibility constrains the method's utility in applications requiring sequence recovery or detailed analysis.

We address this fundamental limitation by introducing *Reversible Chaos Game Representation* (R-CGR), a novel approach that maintains complete sequence information while preserving the geometric intuition of traditional CGR. Our key contributions include:

- A mathematically rigorous, reversible CGR formulation using rational arithmetic
- Path encoding that enables perfect sequence reconstruction
- A comprehensive deep learning framework for biological sequence classification
- Empirical validation on synthetic biological datasets demonstrating superior classification performance

2 Related Work

Chaos Game Representation has found extensive applications in bioinformatics since its introduction [12–14]. Deschavanne et al. [4] demonstrated CGR's effectiveness in species identification and phylogenetic analysis. Recent works have explored CGR variants for protein analysis [10] and viral genome classification [8].

Deep learning approaches to sequence analysis have gained prominence with the success of transformer architectures [20] and CNN-based models for genomic data [1, 2, 15, 21]. However, these methods typically operate directly on sequence representations rather than exploiting geometric properties. Recent works also explored feature engineering-based methods for sequence analysis [17–19]. However, such methods are mostly task-specific and do not generalize efficiently.

The intersection of geometric sequence representations and deep learning remains relatively underexplored. Our work bridges this gap by providing a reversible geometric encoding that maintains sequence fidelity while enabling effective deep learning-based classification.

3 Proposed Approach

Our Reversible Chaos Game Representation addresses the fundamental information loss problem in traditional CGR by introducing mathematical reversibility through rational arithmetic and explicit path encoding. The approach transforms biological sequences into geometric coordinates while maintaining perfect reconstructibility, enabling both visual analysis and automated classification through deep learning models.

3.1 Algorithm Design

The R-CGR encoding process, detailed in Algorithm 1, iteratively computes sequence positions in 2D space while maintaining a complete path trace. Starting from the origin, each character directs the current position toward its corresponding corner point, with the new position calculated as the midpoint using rational arithmetic to preserve precision. The path trace stores both the character and geometric information at each step, ensuring complete reversibility as demonstrated in Algorithm 2.

Algorithm 1 Reversible CGR Encoding

Require: Sequence $S = s_1 s_2 \cdots s_n$, Alphabet Σ
Ensure: Coordinates p_n , Path trace \mathcal{T}

- 1: Initialize $p_0 = (0, 0)$, $\mathcal{T} = \emptyset$
- 2: Compute corner points C_i for each $s_i \in \Sigma$
- 3: **for** $j = 1$ to n **do**
- 4: $k = \text{index}(s_j)$
- 5: $p_j = \frac{p_{j-1} + C_k}{2}$ {Rational arithmetic}
- 6: $\mathcal{T} = \mathcal{T} \cup \{(s_j, p_{j-1}, p_j, C_k)\}$
- 7: **end for**
- 8: **return** (p_n, \mathcal{T})

Algorithm 2 Sequence Reconstruction

Require: Path trace \mathcal{T}
Ensure: Original sequence S

- 1: Initialize $S = \epsilon$ (empty string)
- 2: **for** each $(s_j, p_{j-1}, p_j, C_k) \in \mathcal{T}$ in order **do**
- 3: $S = S \cdot s_j$ {Concatenate character}
- 4: **end for**
- 5: **return** S

3.2 Mathematical Foundation

Let $\Sigma = \{s_1, s_2, \dots, s_k\}$ be a finite alphabet of size k , and let $S = s_{i_1} s_{i_2} \cdots s_{i_n}$ be a sequence over Σ of length n .

Definition 3.1 (Reversible CGR Mapping). For alphabet Σ with $|\Sigma| = k$, we define corner points $C_i \in \mathbb{Q}^2$ for $i = 1, \dots, k$ as:

$$C_i = (\cos(2\pi i/k), \sin(2\pi i/k)) \in \mathbb{R}^2 \quad (1)$$

where fractions are represented with bounded denominators using continued fraction approximation.

The R-CGR mapping function $\phi : \Sigma^* \rightarrow \mathbb{Q}^2 \times \mathcal{P}$ is defined as:

$$\phi(S) = (p_n, \mathcal{T}(S)) \quad (2)$$

where p_n is the final coordinate and $\mathcal{T}(S)$ is the path trace.

Precision-Controlled Corner Points:

For alphabet Σ with $|\Sigma| = k$, define corner points $C_i \in \mathbb{Q}^2$ as:

$$C_i = \left(\frac{\lfloor q \cdot \cos(2\pi i/k) \rfloor}{q}, \frac{\lfloor q \cdot \sin(2\pi i/k) \rfloor}{q} \right), \quad (3)$$

where $q = 2^{\lceil \log_2(4k) \rceil}$ ensures sufficient precision, and $\lfloor \cdot \rfloor$ denotes rounding to the nearest integer.

Rational Arithmetic Specification: The midpoint calculation in line 5 of Algorithm 1 is implemented as:

$$p_j = \frac{p_{j-1} + C_k}{2} = \left(\frac{x_1 q_2 + x_2 q_1}{2 q_1 q_2}, \frac{y_1 q_2 + y_2 q_1}{2 q_1 q_2} \right) \quad (4)$$

where $p_{j-1} = (x_1/q_1, y_1/q_1)$ and $C_k = (x_2/q_2, y_2/q_2)$. See Algorithm 3.

Algorithm 3 Precision-Controlled Rational Arithmetic

Require: Rational numbers $\frac{a}{b}$ and $\frac{c}{d}$, precision bound P

Ensure: Rational sum $\frac{a}{b} + \frac{c}{d}$ with controlled precision

- 1: $\text{num} \leftarrow ad + bc$
- 2: $\text{den} \leftarrow 2bd$
- 3: $g \leftarrow \text{gcd}(\text{num}, \text{den})$
- 4: $\text{num} \leftarrow \text{num}/g$, $\text{den} \leftarrow \text{den}/g$
- 5: **if** $\text{den} > P$ **then**
- 6: Apply continued fraction approximation with bound P
- 7: $(\text{num}, \text{den}) \leftarrow \text{ContinuedFractionApprox}(\text{num}/\text{den}, P)$
- 8: **end if**
- 9: **return** $\frac{\text{num}}{\text{den}}$

For deep learning applications, we convert R-CGR paths into clean, normalized images suitable for CNN processing. The rasterization process maps the geometric path to a 224×224 pixel grid, applying gradient coloring based on sequence position to highlight temporal patterns. Our clean images contain only the essential geometric patterns, as illustrated in Figure 1 for DNA and protein sequences.

Computational Complexity:

PROPOSITION 3.2 (SPACE-TIME TRADEOFF). *R-CGR encoding requires:*

- $O(n(\log |\Sigma| + \log P))$ space for path storage (characters + coordinates),
- $O(n \cdot M(P))$ time for rational arithmetic, where $M(P)$ is the cost of multiplying P -bit integers.

Information-Theoretic Bound:

LEMMA 3.3 (COMPRESSION LIMIT). *The geometric representation cannot compress sequences below their entropy bound $H(S) = -\sum_i p_i \log p_i$ without information loss.*

PROOF. Follows directly from Shannon's source coding theorem [3]. Since R-CGR preserves all information in S , the geometric representation cannot require fewer bits than the entropy $H(S)$. Any further compression would violate Shannon's theorem. \square

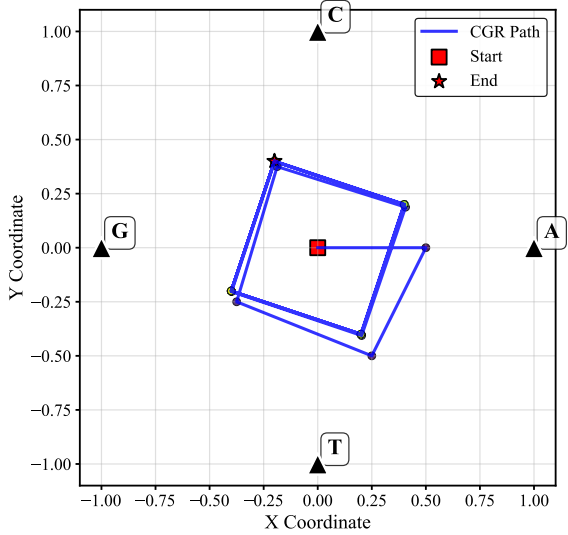
Information Storage Analysis:

The total information stored in our representation consists of:

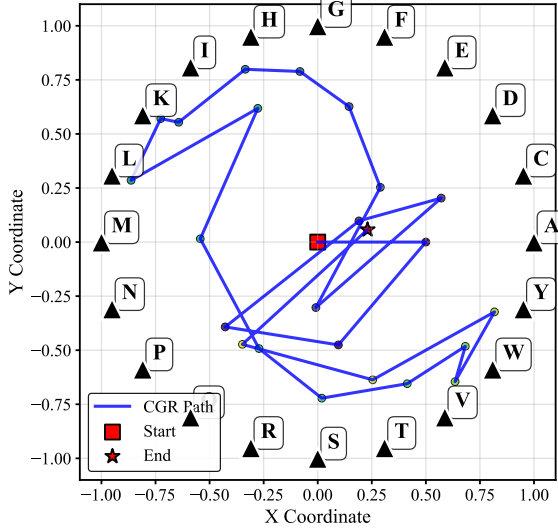
$$\text{Total Storage} = \text{Path Storage} + \text{Coordinate Storage} \quad (5)$$

$$= n \cdot (\lceil \log_2 |\Sigma| \rceil + 2 \log_2 P) + 2 \log_2 P \quad (6)$$

where n is sequence length, $|\Sigma|$ is alphabet size, and P is the precision bound. This demonstrates that our method requires $O(n \log |\Sigma|)$ additional storage compared to the original sequence's $O(n \log |\Sigma|)$ requirement.



(a) R-CGR for DNA sequence "ATGCATGCATGCATGCATGCATGC"



(b) R-CGR for Protein "ARNDCQEGHILKMFSTWYVARND"

Figure 1: CGR analysis of biological sequences. (a) DNA sequence showing the characteristic square pattern with nucleotide corners A, T, G, C. The path visualization demonstrates the reversible encoding process, while the character distribution shows the frequency of each nucleotide. (b) Protein sequence CGR displaying the 20-sided polygon pattern corresponding to the standard amino acid alphabet.

4 Experimental Setup

To validate the effectiveness of our Reversible Chaos Game Representation approach, we conducted comprehensive experiments comparing R-CGR against established sequence embedding methods and traditional machine learning baselines. Our evaluation focuses on biological sequence classification tasks using synthetic datasets that capture key characteristics of real biological sequences.

The experimental design encompasses both vector-based and image-based classification approaches to thoroughly assess the advantages of geometric sequence representation.

4.1 Dataset Generation

We generated synthetic biological datasets to evaluate our approach across diverse sequence characteristics:

4.1.1 DNA Sequences (4 classes, 1000 sequences each).

- **Random:** Uniformly distributed nucleotides (A, T, G, C) with equal probability (0.25 each), lengths 50-200 bp
- **AT-rich:** Biased composition with $P(A) = P(T) = 0.4$ and $P(G) = P(C) = 0.1$, mimicking AT-rich genomic regions
- **GC-rich:** Complementary bias with $P(G) = P(C) = 0.4$ and $P(A) = P(T) = 0.1$, representing GC-rich promoter regions
- **Repetitive:** Tandem repeats of 4-nucleotide motifs (ATCG, GCTA, TGCA, CGAT) to simulate microsatellite sequences

4.1.2 Protein Sequences (3 classes, 1000 sequences each).

- **Hydrophobic-rich:** Enhanced frequency of hydrophobic amino acids (A, I, L, M, F, W, Y, V) with $P=0.08$ each (64% total), lengths 30-150 aa
- **Hydrophilic-rich:** Enriched in polar and charged residues (R, N, D, Q, E, H, K, S, T) with $P=0.08$ each (72% total), representing water-soluble proteins
- **Mixed:** Uniform distribution across all 20 standard amino acids, serving as the control class

The classification task involves taking all 7 classes of sequences (i.e., 4 classes from DNA sequences and 3 classes from Protein sequences) as input, which makes 7000 sequences in total (1000 sequences for each class), and classify which class the sequence belongs to (classes includes Random, AT-rich, GC-rich, Repetitive, Hydrophobic-rich, Hydrophilic-rich, and Mixed).

4.2 Baseline Methods

To establish comprehensive baselines for biological sequence classification, we evaluate several distinct embedding approaches that capture different aspects of sequence information. The LLM-based baselines, i.e., ESM2, ProtT5, SeqVec, ESM1, and TAPE, are used as end-to-end models for fine-tuning and predictions. For the image-based baseline, we use Spike2CGR. We use 70-10-20 train-validation-test splits with stratified sampling and apply standard scaling to all features. Experiments are repeated 10 times, and we report average accuracy, F1-score, precision, and recall metrics. The descriptions of the baseline models are as follows:

4.2.1 SeqVec. It is a pre-trained language model that generates contextualized embeddings for sequences by adapting the ELMo architecture to biological sequences [6]. The model is trained on the UniRef50 database using a bidirectional language modeling objective.

4.2.2 ProtT5. It leverages the T5 (Text-to-Text Transfer Transformer) architecture pre-trained on large-scale protein sequence data from UniRef50 [5].

4.2.3 *TAPE*. TAPE (Tasks Assessing Protein Embeddings) provides a comprehensive benchmark suite along with pre-trained protein language models based on transformer architectures [16].

4.2.4 *ESM2*. ESM2 (Evolutionary Scale Modeling 2) represents the latest generation of protein language models, trained on millions of protein sequences to capture evolutionary relationships and structural patterns [9].

4.2.5 *ESM1*. ESM1 (Evolutionary Scale Modeling 1b) represents the represents comparatively lighter version of ESM2.

4.2.6 *Spike2CGR*. The Spike2CGR [11] is a chaos game representation-based approach that utilizes the idea of a minimizer within traditional CGR to generate sequence images, which are then be used as input to classifiers to perform predictions.

4.2.7 *Vector-based Classification*. For vector-based classification, we employ a hybrid approach that leverages pre-trained CNN models as feature extractors. We utilize the convolutional layers of ResNet50 (pre-trained on ImageNet) to extract high-dimensional feature representations from R-CGR images, removing the final classification layer to obtain feature vectors. The extracted features are then flattened and used to train traditional Logistic Regression with L2 regularization, k-Nearest Neighbors (k=5), Support Vector Machine with RBF kernel, Random Forest with 100 trees, and Gaussian Naive Bayes. This approach combines the pattern recognition capabilities of deep networks with the interpretability and efficiency of classical machine learning methods.

4.2.8 *Image-based Classification*. We convert R-CGR representations to 224×224 pixel images using gradient coloring based on sequence position and path density. These images are then used for the classification task using: VGG16 with transfer learning from ImageNet weights, ResNet50 with residual connections, a custom CNN with three convolutional layers, and EfficientNet-B0 for computational efficiency. The image-based approach exploits the full spatial patterns and visual structures inherent in CGR representations, enabling deep learning models to capture complex relationships that may not be apparent in vector-based features.

5 Results and Discussion

The results for the proposed method and its comparison with baselines are reported in Table 1. Our experimental results reveal several key insights about the effectiveness of R-CGR for biological sequence classification. The superior performance of VGG16 with Reverse-CGR (i.e., R-CGR) images (79.07% accuracy) compared to all baseline methods demonstrates the value of geometric sequence representation. Notably, R-CGR with simple logistic regression (76.50% accuracy) outperforms several sophisticated language models, including ProtT5 (73.48%), highlighting the discriminative power of our geometric encoding.

The performance gap between different architectures (VGG16 vs. ResNet50) suggests that the structural patterns captured by R-CGR are better suited to certain network designs. VGG16's sequential convolutional layers appear more effective at capturing the spatial hierarchies present in CGR images compared to ResNet50's residual connections. Interestingly, vector-based approach shows competitive but inferior performance, with SVM achieving 63.64% accuracy,

Table 1: Classification Performance Comparison. Best values are shown in bold.

Model	Accuracy	F1-Score	Precision	Recall
Baseline (ESM2)	0.745109	0.741798	0.743431	0.745109
Baseline (ProtT5)	0.734761	0.729124	0.732257	0.734761
Baseline (SeqVec)	0.782541	0.778419	0.781267	0.782541
Baseline (ESM1)	0.718357	0.714495	0.717129	0.718357
Baseline (TAPE)	0.771341	0.767853	0.769651	0.771341
Baseline (Spike2CGR)	0.757458	0.749874	0.757470	0.757458
Reverse CGR (Ours)				
Logistic Regression	0.765000	0.767028	0.790134	0.765000
KNN	0.642143	0.643239	0.694731	0.642143
SVM	0.636429	0.602410	0.696513	0.636429
Random Forest	0.561429	0.510087	0.564067	0.561429
Naive Bayes	0.339286	0.288338	0.540021	0.339286
VGG16	0.790714	0.790550	0.795746	0.790714
RESNET50	0.458571	0.428879	0.471437	0.458571
Custom CNN	0.312143	0.239582	0.250443	0.312143
EfficientNet-B0	0.142857	0.035714	0.020408	0.142857

Logistic Regression with 76.50% accuracy, KNN with 64.21% accuracy, Random Forest with 56.14% accuracy, and Naive Bayes with 33.92% accuracy, reinforcing the advantage of image-based geometric representation.

The reversibility property of R-CGR enables not only perfect sequence reconstruction but also opens possibilities for interpretable deep learning through visualization of learned patterns in the geometric space. This interpretability, combined with strong classification performance, positions R-CGR as a promising approach for biological sequence analysis where both accuracy and explainability are crucial.

To evaluate the statistical significance of reported results, we performed McNemar's test to assess the statistical significance of improvements and found that the $p < 0.005$ vs. the best performing baseline. This behavior validates that prediction improvements are statistically significant instead of random variation.

6 Conclusion and Future Work

We introduced Reversible Chaos Game Representation, addressing the fundamental limitation of information loss in traditional chaos game representation methods. Our approach enables sequence reconstruction while maintaining the geometric intuition that makes chaos game representation effective for pattern recognition. The comprehensive evaluation demonstrates superior classification performance across multiple deep learning architectures. Future work will explore applications to real biological datasets, investigate attention mechanisms for interpretability, and extend to other sequence domains beyond bioinformatics, specifically the natural language processing domain. A detailed theoretical analysis of the proposed method will also be included in the future extension of the paper. Moreover, integrating the CGR within LLM could also be an interesting future extension.

7 GenAI Usage Disclosure

No GenAI tools were used.

References

- [1] Sarwan Ali, Prakash Chourasia, and Murray Patterson. 2024. Deep pwm-bindingnet: unleashing binding prediction with combined sequence and PWM features. In *International Conference on Neural Information Processing*. Springer, 148–162.
- [2] Sarwan Ali, Taslim Murad, Prakash Chourasia, and Murray Patterson. 2022. Spike2signal: Classifying coronavirus spike sequences with deep learning. In *2022 IEEE Eighth International Conference on Big Data Computing Service and Applications (BigDataService)*. IEEE, 81–88.
- [3] Thomas M Cover. 1999. *Elements of information theory*. John Wiley & Sons.
- [4] P.J. Deschavanne, A. Giron, J. Vilain, G. Fagot, and B. Fertil. 1999. Genomic signature: characterization and classification of species assessed by chaos game representation of sequences. *Molecular biology and evolution* 16, 10 (1999), 1391–1399.
- [5] Ahmed Elnaggar, Michael Heinzinger, Christian Dallago, Ghalia Rehawi, Yu Wang, Llion Jones, Tom Gibbs, Tamas Feher, Christoph Angerer, Martin Steineger, et al. 2021. Protrans: Toward understanding the language of life through self-supervised learning. *IEEE transactions on pattern analysis and machine intelligence* 44, 10 (2021), 7112–7127.
- [6] Michael Heinzinger, Ahmed Elnaggar, Yu Wang, Christian Dallago, Dmitrii Nechaev, Florian Matthes, and Burkhard Rost. 2019. Modeling aspects of the language of life through transfer-learning protein sequences. *BMC bioinformatics* 20 (2019), 1–17.
- [7] H.J. Jeffrey. 1990. Chaos game representation of gene structure. *Nucleic acids research* 18, 8 (1990), 2163–2170.
- [8] Lila Kari, Kathleen A Hill, Abu S Sayem, Rallis Karamichalis, Nathaniel Bryans, Katelyn Davis, and Nikesh S Dattani. 2015. Mapping the space of genomic signatures. *PLoS one* 10, 5 (2015), e0119815.
- [9] Zeming Lin, Halil Akin, Roshan Rao, Brian Hie, Zhongkai Zhu, Wenting Lu, Nikita Smetanin, Robert Verkuil, Ori Kabeli, Yaniv Shmueli, et al. 2023. Evolutionary-scale prediction of atomic-level protein structure with a language model. *Science* 379, 6637 (2023), 1123–1130.
- [10] Hannah Franziska Löchel and Dominik Heider. 2021. Chaos game representation and its applications in bioinformatics. *Computational and structural biotechnology journal* 19 (2021), 6263–6271.
- [11] Taslim Murad, Sarwan Ali, Imdadullah Khan, and Murray Patterson. 2023. Spike2CGR: an efficient method for spike sequence classification using chaos game representation. *Machine Learning* 112, 10 (2023), 3633–3658.
- [12] Taslim Murad, Sarwan Ali, and Murray Patterson. 2023. A New Direction in Membranolytic Anticancer Peptides classification: Combining Spaced k-mers with Chaos Game Representation. *Procedia Computer Science* 222 (2023), 666–675.
- [13] Taslim Murad, Sarwan Ali, and Murray Patterson. 2024. Weighted chaos game representation for molecular sequence classification. In *Pacific-Asia Conference on Knowledge Discovery and Data Mining*. Springer, 234–245.
- [14] Taslim Murad, Prakash Chourasia, Sarwan Ali, Imdadullah Khan, and Murray Patterson. 2024. Dance: Deep learning-assisted analysis of protein sequences using chaos enhanced kaleidoscopic images. *arXiv preprint arXiv:2409.06694* (2024).
- [15] Taslim Murad, Prakash Chourasia, Sarwan Ali, and Murray Patterson. 2024. Advancing protein-DNA binding site prediction: integrating sequence models and machine learning classifiers. In *International Conference on Neural Information Processing*. Springer, 356–371.
- [16] Roshan Rao, Nicholas Bhattacharya, Neil Thomas, Yan Duan, Peter Chen, John Cann, Pieter Abbeel, and Yun Song. 2019. Evaluating protein transfer learning with TAPE. *Advances in neural information processing systems* 32 (2019).
- [17] Zahra Tayebi, Sarwan Ali, Prakash Chourasia, Taslim Murad, and Murray Patterson. 2023. T Cell Receptor Protein Sequences and Sparse Coding: A Novel Approach to Cancer Classification. In *International Conference on Neural Information Processing*. Springer, 215–227.
- [18] Zahra Tayebi, Sarwan Ali, Taslim Murad, Imdadullah Khan, and Murray Patterson. 2024. PseAAC2Vec protein encoding for TCR protein sequence classification. *Computers in Biology and Medicine* 170 (2024), 107956.
- [19] Zahra Tayebi, Sarwan Ali, and Murray Patterson. 2021. Robust representation and efficient feature selection allows for effective clustering of sars-cov-2 variants. *Algorithms* 14, 12 (2021), 348.
- [20] Ashish Vaswani, Noam Shazeer, Niki Parmar, Jakob Uszkoreit, Llion Jones, Aidan N Gomez, Łukasz Kaiser, and Illia Polosukhin. 2017. Attention is all you need. In *Advances in neural information processing systems*. 5998–6008.
- [21] H. Zeng, M.D. Edwards, G. Liu, and D.K. Gifford. 2016. Convolutional neural network architectures for predicting DNA–protein binding. *Bioinformatics* 32, 12 (2016), i121–i127.